DYNAMICS OF LARGE- AND SMALL-SCALE VORTICAL STRUCTURES IN TURBULENT TAYLOR-COUETTE FLOW

N. Fukushima, T. Fushimi, M. Shimura, M. Tanahashi, and T. Miyauchi
Department of Mechanical and Aerospace Engineering
Tokyo Institute of Technology
2-12-1 Ookayama, Meguro-ku, Tokyo 152-8550, Japan
nfukushim@navier.mes.titech.ac.jp, tfushim@navier.mes.titech.ac.jp,
mshimura@navier.mes.titech.ac.jp, mtanahas@mes.titech.ac.jp,
tmiyauch@mes.titech.ac.jp

ABSTRACT

Direct numerical simulations (DNSs) of turbulent Taylor-Couette flow have been carried out for $Re = 2000 \sim 12000$ to clarify turbulence transition and dynamic characteristics of large vortical structures and fine scale eddies. To investigate effects of the computational domain size, the length of the computational domain in the axial direction is selected to be $4d, 5d$ and $20d$, where d is gap width. At the highest Reynolds number, in addition to fine scale eddies elongated in the azimuthal direction, fine scale eddies parallel to the axial direction are also formed. Dynamic interactions between large- and small-structures are investigated. When the fine scale eddies parallel to the axial direction are strongly stretched in the sweep regions, the fine scale eddies in the azimuthal direction are concentrated in the outflow region near the inner wall and in the inflow region near the outer wall. In contrast, when the fine scale eddies parallel to the axial direction are decreased, the fine scale eddies in the azimuthal direction are expanded. These results suggest that the strength of Taylor vortices is fluctuated temporally and spatially. In the largest computational domain case, the strength of Taylor vortices is fluctuated spatially and Taylor vortices bifurcate and merge at $Re = 8000$. These phenomena are observed only at higher Reynolds numbers. The process of bifurcation and merge of Taylor vortices are also revealed.

Introduction

Taylor-Couette flow is fluid motion between two concentric cylinders where one or both of the cylinders is rotating. Laminar and turbulent Taylor-Couette flow is of great importance in a wide range of engineering applications, such as viscosity measurement devices, rotating machineries and reactors. In this study, we focus on Taylor-Couette flow with a fixed outer cylinder and a rotating inner cylinder. Taylor-Couette flow is one of classical flows to investigate the transition after its instability as is studied firstly by G.I. Taylor (1923). Since then, many theoretical, experimental and numerical researches have been conducted. Taylor-Couette flow changes its flow pattern with the increase of Reynolds number, which has been shown by lots of experimental research (Coles, 1965; Fenstermacher et al., 1979; Larthrop et al., 1992a, b). Quasi-periodicity in the azimuthal direction can be observed in weakly turbulent state and disappears for higher Reynolds number cases (Takeda, 1999; Wang et al., 2005). Measurements of the torque and the scaling exponent α, defined by the dimensionless torque $G \propto Re^{\alpha}$, have been reported in many experimental studies on Taylor-Couette flow with a rotating inner cylinder (Wendt, 1933; Larthrop et al., 1992a, b; Lewis and Swinney, 1999; Racina and Kind, 2006). Reynolds number dependence of the mean torque at the inner cylinder shows a transition at $Re \approx 10000$ (Larthrop et al., 1992a, b). Reynolds number, Re, is defined by gap width (d) and rotating speed of inner cylinder (u_{in}). Recently, only a few of direct numerical simulations of turbulent Taylor-Couette flow have been conducted to investigate the statistical and dy-

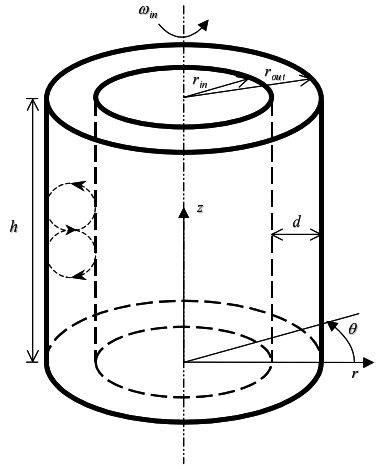

Figure 1. Schematic of the flow geometry.

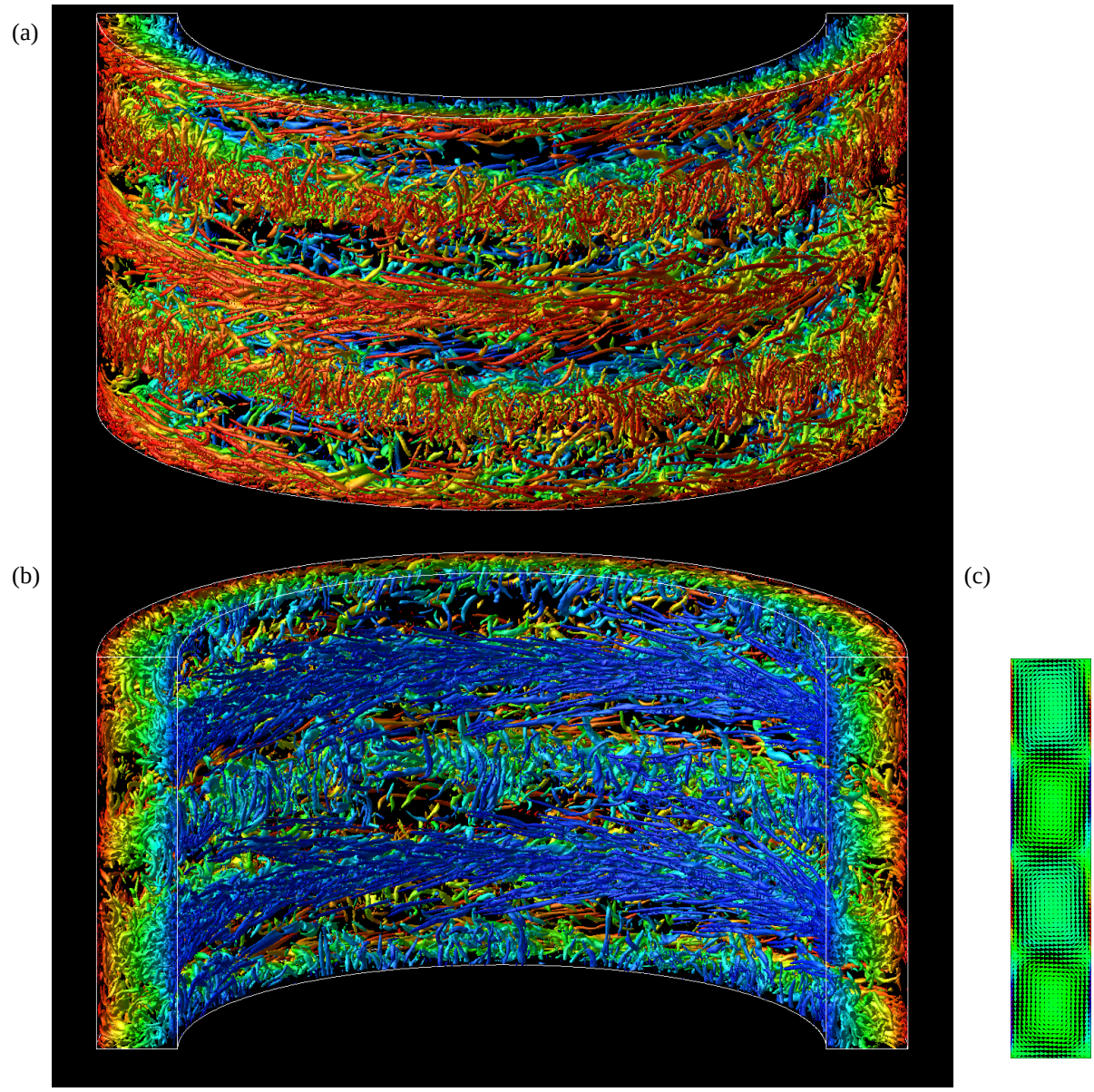

Figure 2. Instantaneous iso-surfaces of the second invariant of velocity gradient tensor from a viewpoint of outer-cylinder side (a) and inner-cylinder side (b) ($Q = 1.0$). Mean velocity vectors in $r-z$ section (c).

namical features (Bilson and Bremhorst, 2007; Dong, 2007). However, turbulence structures in each state have not yet been clarified in detail even for the well-known classical flow.

In this study, DNSs of turbulent Taylor-Couette flow have been carried out for $Re = 2000 \sim 12000$ to clarify turbulence transition and dynamic characteristics of large vortical structures and fine scale eddies.

DNS of Turbulent Taylor-Couette Flow

DNS of Taylor-Couette flow with a fixed outer cylinder and a rotating inner cylinder has been conducted by using Fourier-Chebyshev spectral methods (He et al., 2007). Figure 1 shows the schematic of the flow geometry calculated in the present study. The incompressible Navier-Stokes equations are written in cylindrical coordinate and all variables are normalized by gap width ($d = r_{in} - r_{out}$) and the rotating speed of inner cylinder (u_{in}). The radius ratio ($r* = r_{in}/r_{out}$) is set to be 0.8. The length of the computational domain in the axial direction (h) is selected to be $4d, 5d$ and $20d$. The last one is much larger computational domain than other numerical studies. The length of vortex pair formed in laminar Taylor vortex flow and observed in turbulent Taylor-Couette flow is about $2.0d$ (Taylor, 1923) and $2.5d$ (Burkhalter and Koschmieder, 1974), respectively.

On the wall of both cylinders, no-slip boundary condition is applied. In the axial directions, periodic boundary conditions are assumed. For spatial discretization, spectral method based on Fourier and Chebyshev polynomials has been used. Numerical procedures in Fourier-Chebyshev methods are similar to those of Marcus (1984), and continuity equation is satisfied by applying influence matrix. Gauss-Lobatto points

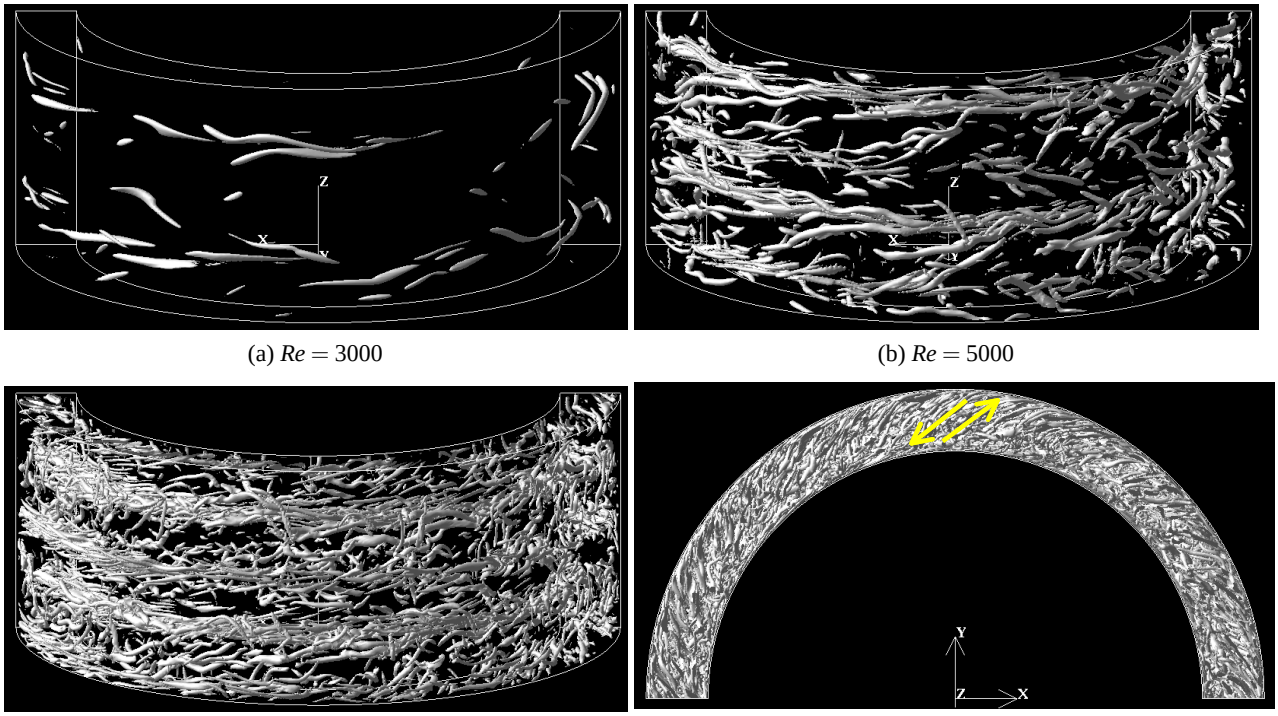

(a) $Re = 3000$ (b) $Re = 5000$

(c) $Re = 8000$ (d) $Re = 12000$, top view

Figure 3. Instantaneous iso-surfaces of the second invariant of velocity gradient tensor ($Q = 1.0$).

are used in the radial direction, which allows fast Fourier transform to obtain Chebyshev polynomials. Fourier spectral methods are employed in other two directions. Time integration is conducted by a three-step time splitting scheme which is composed from 2nd-order Adams-Bashforth scheme for non-linear terms and backward-Euler scheme for other terms. As for initial conditions, the laminar solution of Taylor-Couette flow is added by superposing three-dimensional random perturbation which includes banded white noise. The preliminary calculations are continued until the statistically steady state from the initial conditions. When the flow reaches statistically steady state, the statistical data begin to be obtained. The numerical results of mean torque of the inner cylinder agree with Wendt's empirical formula (Wendt, 1933). $N_r \times N_\theta \times N_z = 97 \times 1280 \times 512$ and $65 \times 864 \times 1280$ grid points are used in the case of $Re = du_{in}/\nu = 12000$ with $h = 5d$ and the case of $Re = 8000$ with $h = 20d$, respectively.

Statistical characteristics and dynamics of large- and small-scale vortical structures

Figure 2 shows iso-surfaces of the second invariant of velocity gradient tensor, $Q = (W_{ij}W_{ij} - S_{ij}S_{ij})/2$, with mean Taylor vortices for the case of $Re = 12000$ and $h = 5d$. Color from blue to red denotes the distance from the wall of the inner cylinder in Fig. 2 (a) and (b). As shown in Fig. 3, the vortical structures in low Reynolds number case ($Re = 3000$) have belt-like distribution in the azimuthal direction with nearly equally spacing in the axial direction. These eddies are formed near the outflow and inflow boundaries. With the increase of Reynolds number, the number of vortical structures increases and those length scale decreases. Fine scale structures exist in almost all regions for high Reynolds number cases. Fine scale eddies possess certain angles with respect to the azimuthal direction near outflow and inflow boundaries. This kind of inclined fine scale eddy is formed due to the mean azimuthal velocity which is higher near the inner cylinder than that near the outer cylinder. For high Reynolds number cases ($Re > 8000$), large scale Taylor vortices include lots of fine scale eddies and seem to organize them. For $Re > 10000$, fine scale structures parallel to the axial direction are formed near the walls. In Fig. 1 (a) and (b), the fine scale eddies parallel to the axial direction are clearly visualized in the sweep regions between neighboring Taylor vortices. This kind of fine scale eddies can be observed only for high Reynolds number cases and is unexpected structure. While fine scale eddies are formed in a stepwise fashion with the increase of Reynolds number, large scale Taylor vortices still persist even for the highest Reynolds number case.

In Fig. 2, fine scale eddies seem to possess different shape and direction. To investigate local characteristics of fine scale eddies, the coherent fine scale eddies (CFSEs) have been identified by the method developed in our previous study (Tanahashi et al., 2004). Spatial distribution of the rotating axis of CFSEs is discussed by introducing inclination angle (ϕ_r) and tilting angle (ϕ_z) of the eddy. Here, ϕ_r is the angle between the tangential direction of the wall and vorticity vector at the CFSE center on $r-\theta$ plane, and ϕ_z is the angle between tangential direction and the vorticity vector on $r-z$ plane. Figure 4 shows joint probability density function (JPDF) of ϕ_r and axial position, and that of ϕ_z and radial position for $Re = 12000$. The peaks of ϕ_r is at about $-40 \sim -50$ and $130 \sim 140$ degree near the outflow and inflow boundaries, which corresponds to the fact that the coherent fine scale

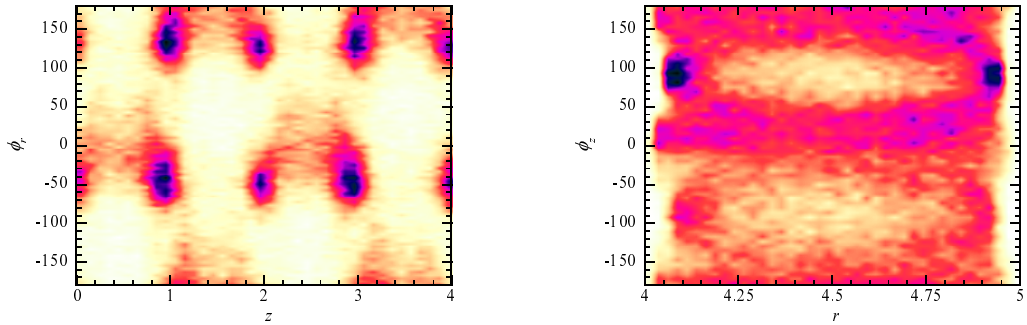

Figure 4. JPDF of the inclination angle and axial position (left) and JPDF of the tilting angle and radial position (right) for $Re = 12000$.

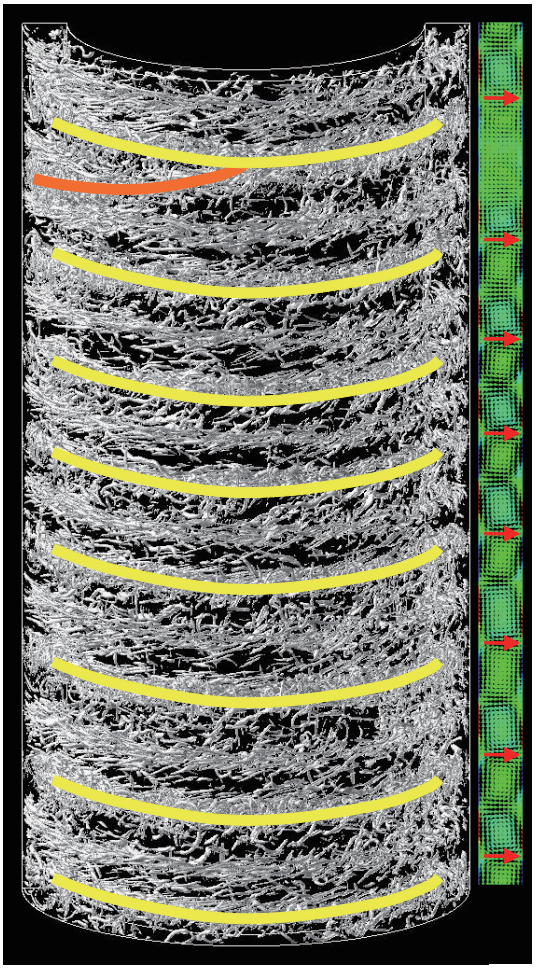

Figure 5. Instantaneous iso-surfaces of the second invariant of velocity gradient tensor for $Re = 8000$ with mean velocity vectors in $r-z$ section.

eddies (CFSEs) have specific angles with respect to the azimuthal direction mentioned above. For $Re = 5000$, ϕ_r near the inflow boundaries is about -50 and 130 degree while ϕ_r near the outflow boundaries is about -40 and 140 degree (not shown here). This is caused by the different distribution of mean azimuthal velocity in the boundaries. For $Re = 12000$, since the mean azimuthal velocity distribution in both boundaries are similar, the peaks of ϕ_r are about -45 and 135 degree near both boundaries. From the JPDF of tilting angle and radial position, it is clear that ϕ_z near the inner and outer walls is close to 90 degree especially for $Re = 12000$. These eddies correspond to CFSEs parallel to the axial direction as shown in Fig. 2. The most expected diameter and the most expected maximum azimuthal velocity of CFSEs are 8η and $1.7u_k$, where η and u_k denote local Kolmogorov length and velocity, for all Reynolds numbers (He et al., 2007). These results coincide with those of other turbulence, such as homogeneous isotropic turbulence, turbulent mixing layer and turbulent channel, which suggests that CFSEs have a universal feature in different turbulent flows.

To reveal dynamic characteristics of these large- and small-scale vortical structures, long-time animations of iso-surfaces of Q in Fig. 2 (a) and (b) have been investigated. The animation files are attached to this paper. Dynamic interactions between these structures are observed in the animations. When the fine scale eddies parallel to the axial direction are strongly stretched in the sweep regions, the fine scale eddies in the azimuthal direction are concentrated in the outflow region near the inner wall and in the inflow region near the outer wall. In contrast, when the fine scale eddies parallel to the axial direction are decreased, the fine scale eddies in the azimuthal direction are expanded. These results suggest that the strength of Taylor vortices is fluctuated temporally and spatially. From the animations, these phenomena have been confirmed.

Bifurcation and merge of turbulent Taylor vortices

The above results are obtained from DNS in smaller computational domain, the axial length of which is $5d$. There is no obvious difference between the results of two computational domains, $h = 4d$ and $5d$. The constraints of the computational domain are strong and there can be only two pairs of Taylor vortices without dependency on Reynolds number. To clarify effects of the computational domain size, DNS results at $h = 20d$ have been investigated. Instantaneous iso-surfaces of the second invariant of velocity gradient tensor, Q, with mean Taylor vortices at $Re = 8000$ are shown in Fig. 5. Fine scale eddies in the azimuthal direction, which have similar characteristics to that for the cases at $h = 4d$ and $5d$, are ob-

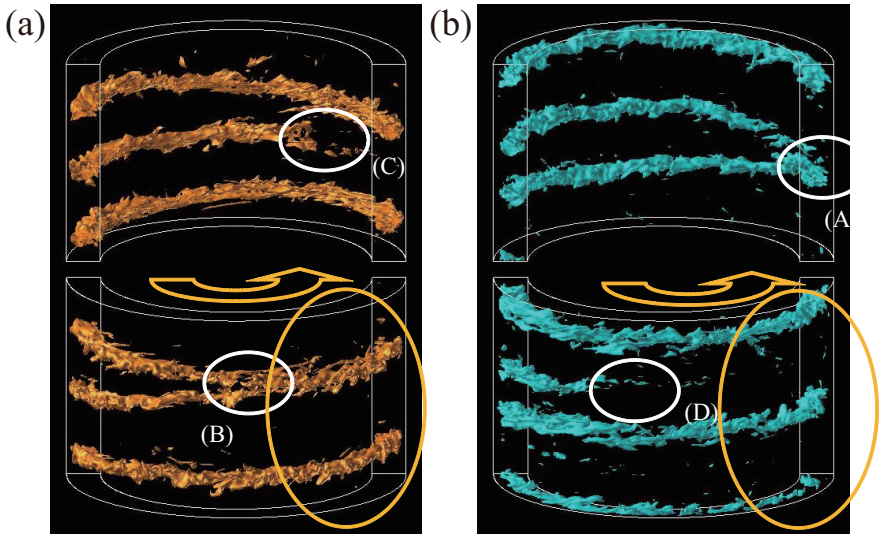

Figure 6. Instantaneous iso-surfaces of radial velocity component for $Re = 8000$ ($u_r = 0.1u_{in}$ (a) and $u_r = -0.1u_{in}$ (b)).

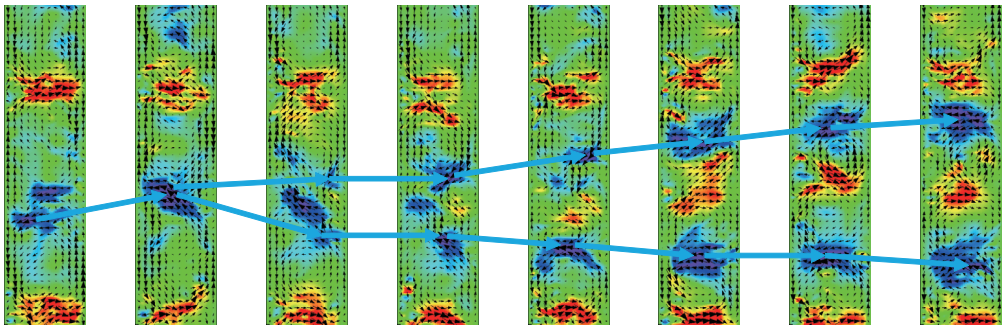

Figure 7. Instantaneous distribution of radial velocity (color; red is outflow and blue is inflow) and velocity vectors in radial-axial planes for $Re = 8000$ (near the bifurcation of inflow).

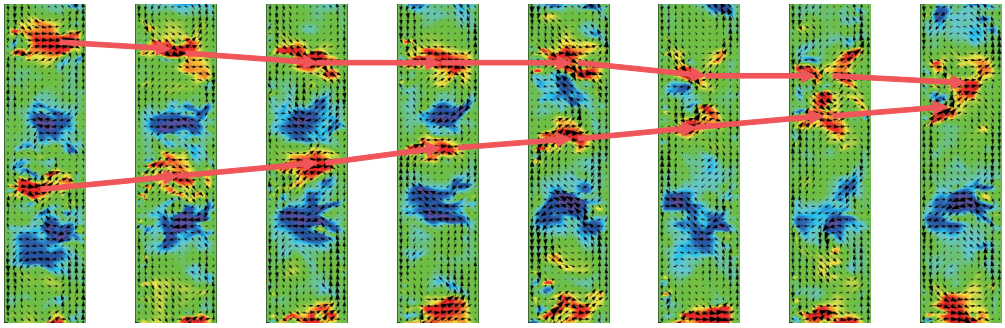

Figure 8. Instantaneous distribution of radial velocity (color; red is outflow and blue is inflow) and velocity fields in radial-axial planes for $Re = 8000$ (near the interflow of outflow).

served. On the other hand, in contrast to the cases at $h = 4d$ and $5d$, averaged number of pairs of Taylor vortices depends on Reynolds number. From the axial energy spectral analysis, there are 9, 10, 8 pairs of Taylor vortices at $Re = 4000, 6000$ and 8000, respectively. They exist with nearly equally spacing in the axial direction at lower Reynolds numbers. However, at $Re = 8000$, as shown in Fig. 5, mean Taylor vortices are weakened and clusters of fine scale eddies near the outer wall, which correspond to the outer flow region, merge in the upper region of the computational domain. These structures are maintained for relatively long time period. These results indicate that the strength of Taylor vortices is fluctuated spatially and that Taylor vortices bifurcate and merge. These phenomena are observed only at higher Reynolds numbers. In experiments, since non-slip wall exists on the top and bottom equipment and it is strong geometrical constraint condition, these bifurcation and merge of Taylor vortices could occur at higher Reynolds number, especially in cases where the axial length of the experimental equipment is far away from integer multiple of the length of a pair of Taylor vortices.

To investigate bifurcation and merge mechanisms of Taylor vortices, outflow and inflow regions at $Re = 8000$ are illus-

trated in Fig. 6 (a) and (b), respectively. A part of the computational domain $(14 \leq z/d \leq 20)$ where bifurcation and merge of Taylor vortices occur is cropped. There are bifurcation of the inflow region (A), merge of the outflow region (B), bifurcation of the outflow region (C) and merge of the inflow region (D). These results suggest number of pairs of Taylor vortices is modulated in the azimuthal direction.

Figure 7 shows instantaneous distribution of radial velocity and velocity vectors in radial-axial planes near the bifurcation of inflow. Here, the right-hand side of the figure corresponds to the outer cylinder, and only the region, $(14 \leq z/d \leq 20)$, is clipped. The gap in the azimuthal direction between figures is $\Delta\theta = \pi/16$. The process of bifurcation of Taylor vortices is as follows. First, the distance between neighboring outflow regions expands and the strength of Taylor vortices between the neighboring outflow regions is weakened. Therefore, the magnitude of velocity decreases in the inflow region. In next, turbulent fluctuations induce instability of the inflow region, divide the inflow region and generate a small outflow region. Finally, the small outflow region is enhanced by centrifugal force and evolves into a fully developed outflow region, and Taylor vortices are bifurcated. In the process of merge of Taylor vortices, the size of the inflow region decreases as the strength of Taylor vortices is weakened gradually, as shown in Fig. 8. Consequently, the neighboring outflow regions merge and finally Taylor vortices also merge.

Conclusions

Direct numerical simulations (DNSs) of turbulent Taylor-Couette flow have been carried out for $Re = 2000 \sim 12000$ based on rotating speed of inner cylinder, u_{in}, and gap width, d, to clarify turbulence transition and dynamic characteristics of large vortical structures and fine scale eddies. To investigate effects of the computational domain size, the length of computational domain in the axial direction is selected to be $4d, 5d$ and $20d$.

In high-Reynolds-number Taylor-Couette flow, many fine scale eddies elongated in the azimuthal direction appear in whole flow fields. At the highest Reynolds number, fine scale eddies parallel to the axial direction are also formed in sweep regions between large scale Taylor vortices. From long-time animations of iso-surfaces of the second invariant of velocity vector tensor, dynamic characteristics of large- and small-scale vortical structures are revealed. When the fine scale eddies parallel to the axial direction are strongly stretched in the sweep regions, the fine scale eddies in the azimuthal direction are concentrated in the outflow region near the inner wall and in the inflow region near the outer wall. In contrast, when the fine scale eddies parallel to the axial direction are decreased, the fine scale eddies in the azimuthal direction are expanded. These results suggest that the strength of Taylor vortices is fluctuated temporally and spatially at the highest Reynolds number.

In contrast to the cases of smaller computational domain, averaged number of pairs of Taylor vortices depends on Reynolds number in the largest computational domain. At $Re = 8000$, mean Taylor vortices are weakened and clusters of fine scale eddies merge in the outer flow region near the outer wall. These structures are maintained for relatively long time period. These results indicate that the strength of Taylor vortices is fluctuated spatially and that Taylor vortices bifurcate and merge. These phenomena are observed only at higher Reynolds numbers. The process of bifurcation and merge of Taylor vortices are also revealed.

REFERENCES

Bilson, M. and Bremhost, K., 2007, "Direct numerical simulation of turbulent Taylor-Couette flow," *Journal of Fluid Mechanics*, Vol.579, pp. 227–270.

Burkhalter, J.E., Koschmieder, E.L., 1974, "Steady supercritical Taylor vortices after sudden starts," *Physics of Fluids*, Vol.17, pp. 1929–1935.

Coles, D., 1965, "Transition in circular Couette flow," *Journal of Fluid Mechanics*, Vol.21 pp. 385–425.

Dong, S., 2007 "Direct numerical simulation of turbulent Taylor-Couette flow," *Journal of Fluid Mechanics*, Vol.587, pp. 373–393.

Fenstermacher, P.R., Swinney, H.L., Gollub, J.P., 1979, "Dynamical instabilities and the transition to chaotic Taylor vortex flow," *Journal of Fluid Mechanics*, Vol.94 pp. 103–128.

He, W., Tanahashi, M., and Miyauchi, T., 2007, "Direct numerical simulation of turbulent Taylor-Couette flow with high Reynolds number," *European Turbulence Conference*, Vol. 11, pp. 215–217.

Lewis, G.S. and Swinney, H.L., 1999, "Velocity structure functions, scaling, and transitions in high-Reynolds-number Couette-Taylor flow," *Physical Review E*, Vol.59, pp. 5457–5467.

Lathrop, D.P., Fineberg, J., Swinney, H.L., 1992a, "Turbulent flow between concentric rotating cylinders at large Reynolds number," *Physical Review Letters*, Vol.68, pp. 1515–1518.

Lathrop, D.P., Fineberg, J., Swinney, H.L., 1992b, "Transition to shear-driven turbulence in Couette-Taylor flow," *Physical Review A*, Vol.46, pp. 6390–6405.

Marcus, P.S., 1984, "Simulation of Taylor-Couette flow. Part 1. Numerical methods and comparison with experiment," *Journal of Fluid Mechanics*, Vol.146, pp. 45–64.

Racina, A. and Kind, M., 2006, "Specific power input and local micromixing times in turbulent Taylor-Couette flow," *Experiments in Fluids*, Vol.41, pp. 513–522.

Tanahashi, M., Kang, S.J., Miyamoto, T., Shiokawa, S., Miyauchi, T., 2004, "Scaling law of fine scale eddies in turbulent channel flows up to Re_τ=800," *International Journal of Heat and Fluid Flow*, Vol. 25, pp. 331–340.

Takeda, Y., 1999, "Quasi-periodic state and transition to turbulence in a rotating Couette system," *Journal of Fluid Mechanics*, Vol.389, pp. 81–99.

Taylor, G.I., 1923, "Stability of a viscous liquid contained between two rotating cylinders," *Philosophical Transactions of the Royal Society of London. Series A*, Vol. 223, pp. 289–343.

Wang, L., Olsen, M.G., Vigil, R.D., 2005, "Reappearance of azimuthal waves in turbulent Taylor-Couette flow at large aspect ratio," *Chemical Engineering Science*, Vol.60, pp. 5555–5568.

Wendt, F., 1933, "Turbulente Stromungen zwischen zwei rotierenden konaxialen Zylindern," *Archive of Applied Mechanics*, Vol.4, pp. 577–595.